

Table 1 Elemental and isotopic compositions of rare gases in diamond

Sample	Batch 1		Blank 1		Batch 2		Blank 2	
Weight (g)		1.98			2.61			
Temperature (°C)	800	2,000	2,100	2,000	800	2,000	2,100	2,000
Time of heating (min)	30	60	5	60	30	60	60	60
$^3\text{He} \times 10^{-13} \text{ cm}^3 \text{ g}^{-1} \text{ (STP)}$	<3	286	<10	<20	<10	179	<10	<20
$^4\text{He} \times 10^{-9}$	1.36	3480	0.09	1.1	1.57	918	0.37	2
$^{20}\text{Ne} \times 10^{-12}$	6.3	20.7	<0.1	20	2.1	10.2	<0.1	20
$^{36}\text{Ar} \times 10^{-11}$	3.35	36.7	10	2.4	1.54	9.37	1.90	2
$^{84}\text{Kr} \times 10^{-12}$	1.8	3.6	<0.02	0.6	1.0	2.9	0.26	0.8
$^{132}\text{Xe} \times 10^{-13}$	3.5	9.1	<2	2	4.4	7.3	1.0	2
$^3\text{He}/^4\text{He}$	$<2 \times 10^{-4}$	$(8.23 \pm 0.35) \times 10^{-6}$				$(1.95 \pm 0.07) \times 10^{-5}$		
$^{40}\text{Ar}/^{36}\text{Ar}$	359 ± 2	436 ± 2			574 ± 14	$1,121 \pm 8$		
$^{128}\text{Xe}/^{132}\text{Xe}$		0.0754 ± 0.0011				0.0718 ± 0.0037		
$^{129}\text{Xe}/^{132}\text{Xe}$		0.996 ± 0.019				0.978 ± 0.004		
$^{130}\text{Xe}/^{132}\text{Xe}$		0.161 ± 0.007				0.149 ± 0.006		
$^{131}\text{Xe}/^{132}\text{Xe}$		0.786 ± 0.023				0.779 ± 0.014		
$^{134}\text{Xe}/^{132}\text{Xe}$		0.391 ± 0.012				0.386 ± 0.009		
$^{136}\text{Xe}/^{132}\text{Xe}$		0.328 ± 0.012				0.318 ± 0.018		

Other isotopic ratios are indistinguishable from atmospheric values

rare gases observed in batch 2 may be representative of those carried by CO_2 phase, whereas rare gases in batch 1, or more specifically rare gases in the black inclusions, is rather indicative of a region where the diamonds occluded the former.

Ar isotopic ratios observed in diamonds do not seem to support the speculation¹⁰ that diamonds were formed from materials in subducting ocean sediments, since even very small amount of seawater contamination (say less than 0.1%) which would necessarily accompany ocean sediments would reduce $^{40}\text{Ar}/^{36}\text{Ar}$ isotopic ratio to almost atmospheric value (295.5) because of relatively very high Ar content (about 0.03%) in seawater. The observed $^{40}\text{Ar}/^{36}\text{Ar}$ is much higher than the atmospheric ratio, ruling out any noticeable amount of seawater contamination.

NOBUO TAKAOKA

Department of Physics,
Osaka University,
Toyonaka 560, Japan

MINORU OZIMA

Geophysical Institute,
University of Tokyo,
Tokyo 113, Japan

Received 2 August; accepted 4 November 1977.

- Ozima, M. *Geochim. cosmochim. Acta* **39**, 1127-1134 (1975).
- Schwarzman, D. W. *Nature Phys. Sci.* **245**, 20 (1973).
- Tolstikhin, I. N. *Earth planet. Sci. Lett.* **26**, 88-96 (1975).
- Boulos, M. S. & Manuel, O. K. *Science* **174**, 1334-1336 (1971).
- Melton, C. E. & Giardini, A. A. *Am. Mineral.* **59**, 775-782 (1974).
- Melton, C. E. & Giardini, A. A. *Nature* **263**, 309-310 (1976).
- Sharp, W. E. *Nature* **211**, 402-403 (1966).
- Takaoka, N. *Mass Spectrosc.* **24**, 73-86 (1976).
- Craig, H. & Lupton, J. E. *Earth planet. Sci. Lett.* **31**, 369-385 (1976).
- Frank, F. C. in *Sci. Technol. Ind. Diamonds* **1** (1967).

On melting icebergs

THE feasibility of towing icebergs to their coasts and melting them on arrival to provide a supply of fresh water is being studied in various parts of the world. Saudi Arabia, Australia and California¹ are amongst those considering such a project. One suggestion for melting the icebergs is to run each iceberg aground in water approximately 250 m deep, the mean depth of Antarctic icebergs. A relatively shallow pen would then be built around the iceberg and it is conjectured that the melt water will rise, without much mixing, into the pen, from where it will be siphoned off for subsequent use. Neshyba² claims, however, that melt water produced by icebergs may be responsible for a large amount of upwelling and mixing in the Antarctic's Weddell Sea. He asserts that as the melt water rises up the side of an iceberg, it entrains a sizeable quantity of warmer, saltier water from

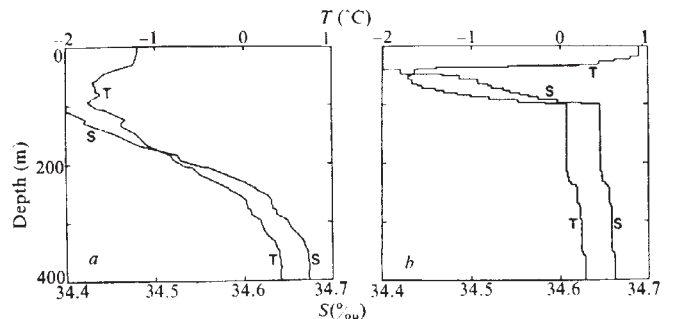


Fig. 1 Temperature (T) and salinity (S) profiles measured in the upper 400 m of the Weddell Sea (adapted from Fig. 3 of Foster and Carmack³). a , Near the Scotia Ridge at the northern edge of the Sea; b , near the turning point of the current gyre.

the environment. Neshyba calculates that an average-sized iceberg is thus responsible for a vertical volume transport into the upper layer of the Weddell Sea of $3.3 \times 10^8 \text{ cm}^3 \text{ s}^{-1}$. This is a considerable transport, and the raising of water and nutrients from depth by this mechanism would be of importance in determining the physical and biological properties of the Weddell Sea. The first suggestion, that fresh melt water rises to the surface, and Neshyba's claims that the melt water will have mixed significantly with its salty environment before reaching the surface, cannot both be correct. We show here that both may be in error.

The vital fact neglected in both arguments is that the ocean environment is not only salty, but there is also a salinity gradient in the upper 250 m of most areas of the oceans. For example, data from the Weddell Sea shown in Fig. 1 (taken from Foster and Carmack³) indicate that the salinity increases with depth, as does the temperature in this region. The data indicate further that both the salinity and temperature distribution have a characteristic 'stepped' structure, with layers of well mixed temperature and salinity separated by sharp interfaces in which both properties vary more rapidly. Similarly, off the Californian coast the salinity again has a general increase with depth, while there is an overall decrease in temperature (see, for example, Gregg and Cox⁴, in particular their Fig. 1). We have carried out a series of experiments in which ice is inserted into a salinity gradient, and the preliminary results are reported here.

Iceblocks made from water which had been deaerated under vacuum measuring approximately $20 \text{ cm} \times 10 \text{ cm} \times 3 \text{ cm}$ were inserted vertically (see Figs 2-3) into salt-stratified water at room temperature ($\sim 23^\circ \text{C}$) with constant density gradients of between 1×10^{-3} and $6 \times 10^{-3} \text{ g}$

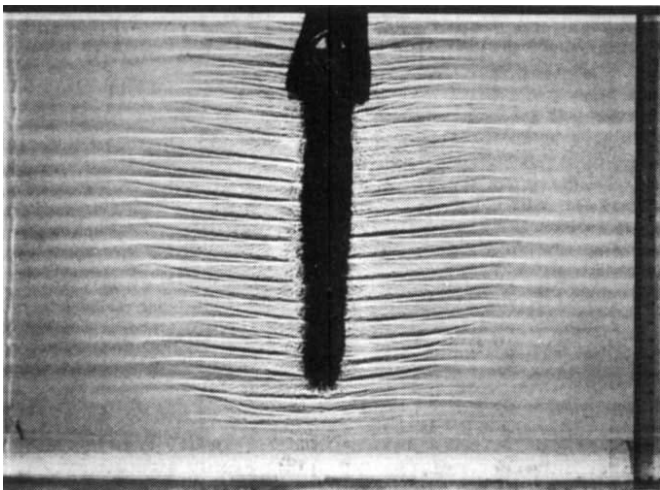


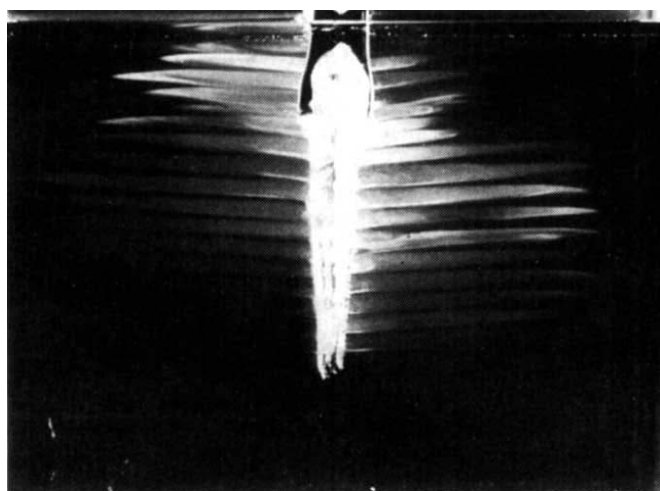
Fig. 2 Shadowgraph photograph showing the tilted layers and interfaces produced by inserting a block of ice into salt-stratified water at room temperature. (Specific gravity at top of tank 1.00, and at bottom 1.05; depth 26 cm.)

cm^{-3} per cm and surface densities between 1.00 and 1.10 g cm^{-3} .

Adjacent to the ice, melt water at 0°C rises in a thin, generally turbulent boundary layer until its density equals that of the surroundings at the same level. Above the level where these densities are equal the melt water in the boundary layer sinks. In our experiments this level occurs at a density of approximately 1.01 g cm^{-3} (if this exists), although in the ocean, with its typically lower temperature and higher salinity, such a level (where the density of the fresh melt water equals that of its surroundings) is unlikely to occur. The presence of a horizontal temperature gradient imposed upon the existing vertical salinity gradient alters the boundary layer a small distance away from the ice, producing a regular series of tilted convecting layers which grow out into the environment, as shown in Figs 2–4.

These layers exist because of double-diffusive convection, which readily occurs whenever two components of different molecular diffusivities contribute to the density. The general principles governing this form of convection and some applications are discussed by Turner⁵. Along the bottom of each layer, relatively fresh, cold water acquires heat and some

Fig. 3 An experiment carried out using the same conditions as shown in Fig. 2, but with fluorescein frozen into the ice block, and side illumination. The spread of the dye again shows the layers, but also indicates the distribution of the melt water.



salt across the 'diffusive' interface separating it from the environmental water at the top of the layer below. Thus the melt water becomes progressively lighter and runs uphill as indicated by the upward tilt of the layers seen in Figs 2–3. Along the top of the layers there is an inflow of environmental fluid, which is directly mixed with the melt water only near the ice. In this way a considerable portion of the melt water can be fed into the environment close to the level at which it is produced and very little, if any, rises to the surface.

The melting rate of the ice is controlled by the rate of heat transfer from the environment, and is thus greatly influenced by the circulation that occurs. On a large scale this means that increasing the salinity of the environmental fluid increases the relative buoyancy of the melt water.

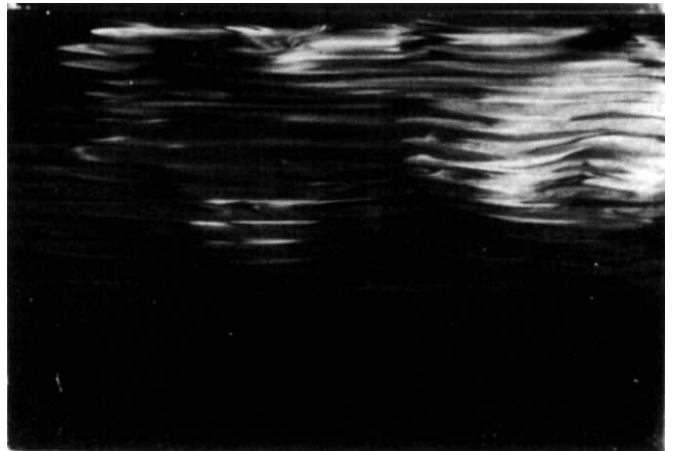


Fig. 4 The experimental tank at a later stage of the experiment of Fig. 3, soon after the iceblock had been carefully removed. The volume of dyed water is much greater than that of the ice block, indicating that the melt water mixes with a large volume of salty water and spreads out close to the level at which it is produced; little reaches the surface.

The velocity in the boundary layer thus increases, which results in increased melting. On a smaller scale, the layered motion produces a series of horizontal ridges (see Fig. 5) along the sides of the ice, with the deepest erosion corresponding to the centre of each of the layers, and the ridges to the interfaces between them. In each experiment, the layer size is reasonably uniform with depth and increases with either decreasing density gradient or increasing central salinity. In the laboratory this size is of the order of 1 cm. In the Antarctic, the weaker salinity gradients will tend to make the layers deeper, though this will be counteracted by the smaller horizontal density gradients. The quantitative scaling relations are to be discussed elsewhere.

Further suggestions follow immediately from the results of these experiments. First, the data displayed in Fig. 1*b* were obtained near the centre of the large gyre which characterises the circulation in the Weddell Sea. This structure differs markedly from that at the edges of the gyre (Fig. 1*a*) in that it has much stronger temperature and salinity gradients from 50–100m depth, weaker density gradients from 50–500 m and a more clearly defined step structure. We conjecture that this difference is due to the systematic injection of melt water at intermediate depths by icebergs which spend a longer time near the centre of the gyre. The spatial variability of the layering in this region³ is consistent with such a localised mechanism of formation, rather than a more extensive 'one-dimensional' convection process acting over the whole area.

Further measurements of temperature and salinity, made as close as possible to an iceberg in order to detect the layering, would be instructive. It would then be worthwhile

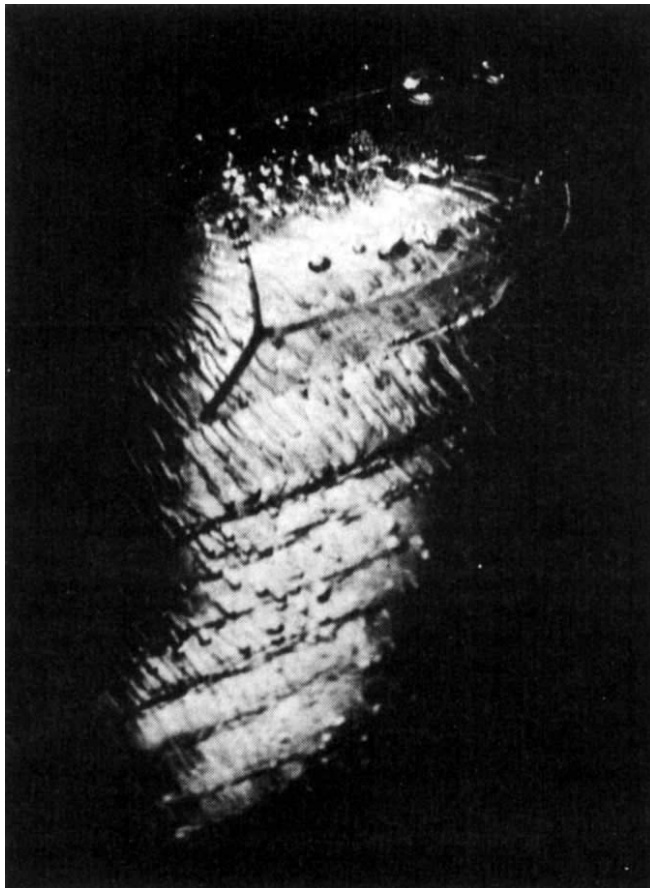


Fig. 5 An oblique view of a melting ice block, taken through the water surface. Note the ridges, caused by the uneven melting associated with the convection in layers.

exploring the structure of the layers as a function of distance from the ice. A direct search for the ridges associated with the variation in rate of melting produced by the convection might also be considered.

Finally, our results imply that those seeking to obtain fresh water from icebergs will have to consider alternative methods which isolate the melt water in some way from the surrounding seawater.

We thank R. Wylde-Browne for his able assistance with the experiments and particularly with the photography. This research was carried out while H.E.H. was a visiting fellow at the Australian National University and was in part supported by grants from the Royal Society and the British Admiralty.

HERBERT E. HUPPERT

*Department of Applied Mathematics
and Theoretical Physics,
Silver Street,
Cambridge, UK*

J. STEWART TURNER

*Research School of Earth Sciences,
Australian National University,
Box 4, Canberra, Australia*

Received 21 September; accepted 3 November 1977.

1. Agarwal, A. *New Scientist* 75, 11–13 (1977).
2. Neshyba, S. *Nature* 267, 507–508 (1977).
3. Foster, T. D. & Carmack, E. C. *J. phys. Oceanogr.* 6, 36–44 (1976).
4. Gregg, M. C. & Cox, C. S. *Deep-Sea Res.* 19, 355–376 (1972).
5. Turner, J. S. *Buoyancy Effects in Fluids* (Cambridge, 1973); *A. Rev. fluid Mech.* 6, 37–56 (1974).

Iceberg sounding by impulse radar

KNOWLEDGE of an iceberg's draft is essential for assessing its risk to underwater installations, in predicting its drift, and for estimating its total bulk. Because of the highly irregular shape of icebergs, it is impossible to estimate an iceberg's draft directly from its above-water dimensions. Large tabular icebergs have been sounded using radio techniques^{1,2}. We report here that estimates of the draft of irregularly-shaped icebergs can also be obtained from the air quickly and accurately using short-pulse radar. A small iceberg in Twillingate Harbour, Newfoundland (49° 40'N, 54° 46'W) was sounded from a helicopter using impulse radar, on 11 June 1977. The result was verified by simultaneous measurement of the iceberg's draft using side-scan sonar.

The impulse radar equipment¹, built by Geophysical Survey Systems consists of a control unit and an FM tape recorder, which were mounted in a helicopter, and a transmitter-receiver and antenna assembly, which was slung in a net about 6 m beneath the aircraft. The radiation pattern of the antenna is similar to that of a half-wave dipole. The transmitted signal is a broad-band pulse with a duration of about 20 ns and a centre frequency near 80 MHz. The receiver was set to accept echoes for up to 1.4 μ s, and by sequential sampling of the received signal, an audio-frequency replica trace was constructed and recorded on tape. After sampling, the effective repetition rate was 51.2 scans s^{-1} .

One of the impulse radar records is shown in Fig. 1, taken with the aircraft flying approximately 20 m above sea level. Strong echoes are represented by dark lines; signals received with long delay time are enhanced by a time-gain amplifier. Initial returns are due to reflections of the transmitted pulse between the antenna and the helicopter. The echo from the sea surface is very clear, but, as the iceberg is approached, this echo fades and a faint return from the sharply-peaked top of the iceberg is seen. Reflections from within the iceberg are very clear, although there is no unique bottom echo, since the radar signal reverberates within the iceberg. A set of multiple echoes is received with longer delay time.

To interpret the iceberg draft, the speed of the radar pulse in ice must be known. The speed of electromagnetic waves travelling in a dielectric medium is given by $c\epsilon_r^{-1/2}$, where c is the speed of light in free space, and ϵ_r is the relative dielectric constant of the medium. A dielectric constant of 3.2 was used, giving a velocity of 0.084 $m\ ns^{-1}$ of two-way travel time in ice. Ice samples collected from the iceberg surface were polycrystalline, and had a density of $0.938 \pm 0.011\ Mg\ m^{-3}$. These values for density and dielectric constant are consistent with previous work³.

The travel time used to interpret the draft was that from the first subsurface echo that was received directly beneath the centre of the iceberg. This return represents the most direct route through the ice, and it had a consistent multiple. Of course, there is no guarantee that this return came from the deepest subsurface point of the iceberg. The average draft of the iceberg was estimated to be $18.0 \pm 0.9\ m$, with a standard deviation of 0.7 m over 16 passes. The height of the iceberg was also estimated, giving a draft: height ratio of about 4.3:1.

The hyperbolic patterns seen on either side of the iceberg are interpreted as reflections from pulses which entered the upper side of the iceberg, and traversed the iceberg before returning. Their path length in the ice was greater than the direct top-to-bottom path length, and the hyperbolic pattern is caused by the increased path length in the air as the horizontal helicopter-iceberg separation increased. These hyperbolic returns are often stronger than the direct bottom return as a larger proportion of the signal incident on the